Int. J. Heat Mass Transfer. Vol. 34, No. 6, pp. 1451–1464, 1991
Printed in Great Britain

0017–9310/91 $3.00 + 0.00

Statistical investigation of the relationship between interfacial waviness and sensible heat transfer to a falling liquid film

T. H. LYU and I. MUDAWAR
Boiling and Two-phase Flow Laboratory, School of Mechanical Engineering,
Purdue University, West Lafayette, IN 47907, U.S.A.

(*Received* 6 *April* 1990 *and in final form* 10 *July* 1990)

Abstract—Experiments are performed to provide an insight into the heat transfer aspects of a wavy liquid film. Local film thickness and liquid temperature are measured simultaneously using a thermal conductance thickness probe and fast response thermocouples as the wavy film falls over an electrically heated wall. Liquid temperature at a fixed distance from the wall generally increases in the thin substrate portion of the film and decreases within the large waves. Temperature shows complex excursions within the large waves due to turbulent eddies and to the relative liquid motion between the large wave and the surrounding substrate. The measurements are examined with the aid of statistical tools to investigate the relationship between film thickness and liquid temperature at various film Reynolds numbers and heat fluxes. The correlation between the two variables is stronger at higher heat fluxes compared to lower fluxes. A cross-spectrum analysis shows a distinct band of dominant frequencies in the relationship between the two variables.

1. INTRODUCTION

UNDERSTANDING the transport characteristics of liquid films is of great practical importance in many industrial applications such as thin film evaporators, plate-type condensers, distillation columns, gas absorption equipment and cooling hardware for high-power computer chips.

At flow rates of industrial interest, falling liquid films may be turbulent and characterized by the formation of waves at the film interface. Understanding the effects of these waves is very important in predicting the heat and mass transfer coefficients in falling film devices because of the enhancement in heat and mass transfer rates attributed to these waves [1, 2]. The stochastic nature of these waves has been largely responsible for the difficulty in modelling turbulent liquid films. Although extensive work has been reported in the literature on the mechanisms of film instabilities [3–9] and on the time averaged heat transfer coefficient across the film [1, 2, 10–14], there exists a particular need for experimental data for the local instantaneous temperature profile within advancing film waves, information essential to the understanding and modelling of wavy film flow. One reason for the lack of such data is the difficulty in experimentally measuring the temperature within a falling film due to the small film thickness (~ 1 mm) and to the relatively high frequency of interfacial waves on a typical film.

A few investigators used numerical techniques to predict the hydrodynamic structure of a wavy falling film. Maron *et al.* [15] verified the existence of interfacial stagnation points and identified regions of recirculation and flow reversal in the motion of liquid within a large solitary wave relative to the wave itself. Wasden and Dukler [16, 17] illustrated how interaction between adjacent waves significantly modifies the flow field compared to solitary waves. Unfortunately, these numerical studies have been limited to adiabatic, laminar films with Reynolds numbers near 1000.

Several studies have shown a significant impact of waviness on the transport phenomena associated with liquid films. Miya *et al.* [18] measured the variation of wall shear stress with film thickness in horizontal co-current gas–liquid flow. They detected a sudden relaxation of the shear stress upstream of the wave and a sharp increase in the front region within the wave. Similar results were also reported for falling films by Wasden and Dukler [16, 17]. Brauner and Maron [19] measured maximum mass transfer rates between a liquid film and a wall just downstream from wave peaks.

Recently, Ganchev and Trishin [20] published their findings on a study the objectives of which are closely related to those of the present. They measured film thickness and wall and liquid temperatures simultaneously for water films having low flow rates (0.2–2 kg m^{-1} s^{-1}) subjected to heat fluxes ranging from 1×10^5 to 5×10^5 W m^{-2}. Film thickness was measured by a conductance probe while the wall and liquid temperatures were measured using only one thermocouple in each region. Their data showed a sharp drop in liquid temperature concurrent with the arrival of a large wave, followed by an increase in liquid temperature upstream of the next large wave. This observation is consistent with the results of other thin film transport studies concerning the fluctuations

NOMENCLATURE

Bi	Biot number, $h_b D_b/6k_b$
c	specific heat
$C(\tau)$	cross-covariance function
D_b	thermocouple bead diameter
f	frequency
h_b	convection heat transfer coefficient for cross flow of liquid over a spherical thermocouple bead
k_b	thermal conductivity of thermocouple bead
n	number of samples in a subset of the data record
N	total number of samples in a data record
$p(s)$	probability density function
$P(s)$	probability distribution function
Pr	Prandtl number
q	heat flux
$R(\tau)$	autocovariance function
Re	Reynolds number, $4\Gamma/\mu$
$s(t)$	random variable
$S(f)$	autospectrum function
t	time
T	liquid temperature
V_w	wave velocity
$W(f)$	cross-spectrum function
y	distance from the solid wall.

Greek symbols

Γ	mass flow rate per unit film width
δ	instantaneous film thickness
μ	dynamic viscosity
σ^2	variance (second central moment)
ρ	density
τ	time lag in correlation functions
τ_s	total sampling period
$\tau_{t,b}$	thermal time constant of thermocouple bead, $\rho_b c_b D_b/6h_b$.

Subscripts

b	thermocouple bead
min	minimum
s	surface
w	wall.

Superscript

$\bar{}$	average value; time mean.

of mass transfer rate [19] and wall shear stress [16–18] with film thickness.

This paper aims at developing some understanding of the heat transfer characteristics of wavy films. Experimental data for the instantaneous temperature profile measured simultaneously with film thickness are discussed qualitatively and analyzed statistically to provide insight into the relationship between interfacial waves and heat transfer to a falling water film.

2. EXPERIMENTAL APPARATUS AND PROCEDURES

The present study utilized an experimental apparatus described in previous papers [1, 2]. The apparatus

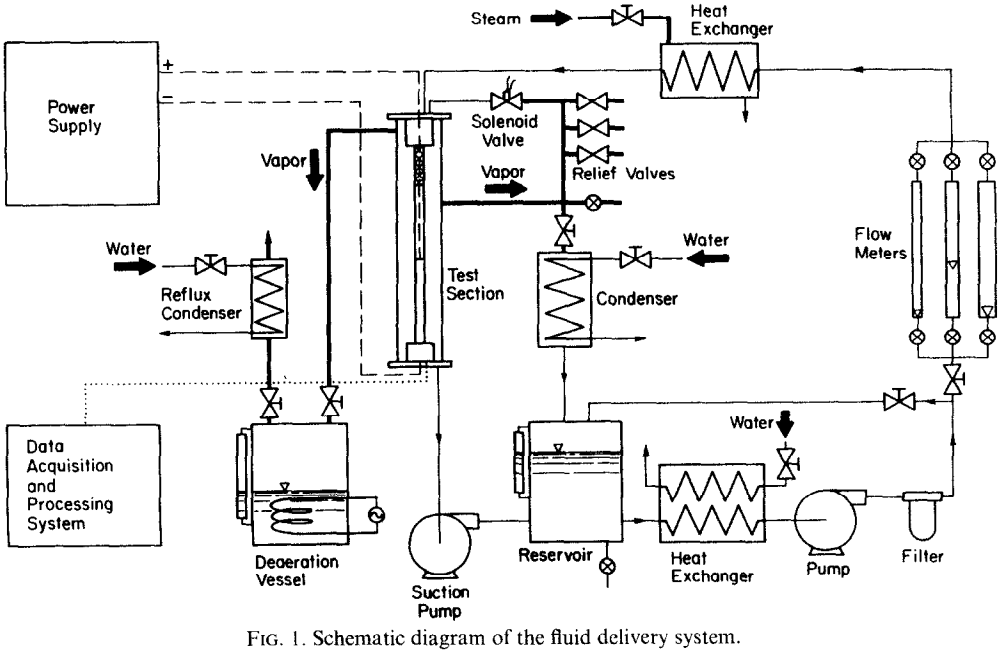

FIG. 1. Schematic diagram of the fluid delivery system.

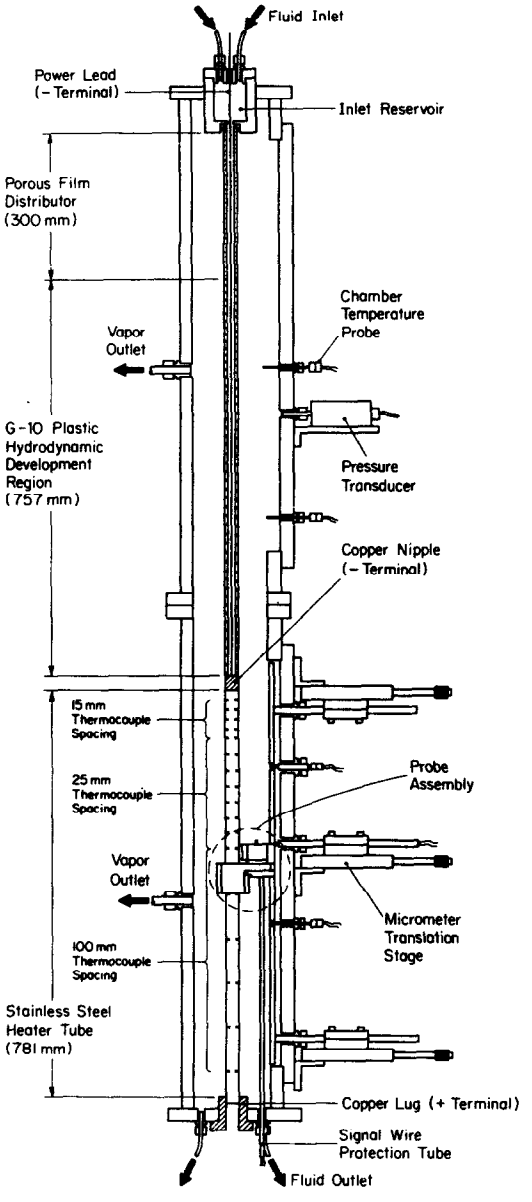

FIG. 2. Cut-away view of the test chamber.

was modified with new film thickness probes, temperature probes, and probe assembly handling devices. A schematic of the test chamber, fluid delivery system and other auxiliary components is shown in Fig. 1. The test fluid used in the present study was deionized water which was replaced at least every 4 h of system operation. The liquid film was formed on the outside wall of a 25.4 mm diameter, 1835 mm long test section. The test section was composed of a polyethylene porous film distributor, a 757 mm long G-10 fiberglass plastic hydrodynamic development section and a thin stainless steel heated test section 781 mm long as displayed in Fig. 2. The wall heat flux was generated in the stainless steel section by a low voltage, high d.c. current (up to 15 V at 750 A). Data presented in this paper were measured at a location 278 mm below the top of the stainless steel heater tube, outside the thermal entrance region determined experimentally in ref. [1].

Figure 3 shows a detailed diagram of a probe assembly block which positioned the delicate temperature and thickness probes. The probe block was centered around the heater by six alignment screws. Longitudinally, the block was positioned along a guide rail at any desired vertical location. Horizontal movement of the block was controlled by two micrometer translation stages attached to the guide rail. Twelve thermocouples were installed over a 5 mm span on the knife edge of the probe assembly block to measure the temperature distribution across the film as shown in Fig. 4. The most critical task in instrumenting the knife-edge assembly was the mounting of individual thermocouple beads and the routing of very closely spaced wires to external leads. This task was accomplished with the aid of a microscopic lens, by positioning the bead of the thermocouple closest to the heated wall in place and coating its wires on either side of the knife edge with a thin layer of epoxy. This process was repeated for each of the twelve thermocouples. Several knife-edge probes failed during assembly and the entire knife edge had to be re-instrumented due to contact between wires of adjacent beads, or to the breaking of individual thermocouples near the bead. In the test chamber, the knife edge was protected against damage due to forced contact with the wall by a contact plane protruding from the downstream side of the knife edge. The G-10 fiberglass material of the knife edge combined the attractive features of low thermal conductivity, high dielectric strength and high mechanical strength. A thickness probe and a probe for calibrating the thickness probe were both installed in the same horizontal plane as the thermocouples. A second thickness probe was located 29.7 mm downstream in the vertical direction and 41 deg in the circumferential direction from the upper thickness probe. The second thickness probe (which was not used in the present study) facilitated measurement of the wave velocity between the two probe locations.

Thermocouples on the knife edge were made from type-E chromel and constantan 0.0508 mm diameter wire. The thermocouple beads had an estimated thermal time constant of 0.39 ms $\leqslant \tau_{t,b} \leqslant$ 0.55 ms and a Biot number of $0.05 \leqslant Bi \leqslant 0.07$ in water at typical film velocities. The maximum standard deviation of temperature fluctuation for each thermocouple was 0.17°C which was caused by the high speed data acquisition system itself. The thermocouples were calibrated in a constant temperature bath at several temperatures. The probe assembly block was then positioned around the heater and the lower part of the test chamber was filled with water to a level above the probe assembly block. The heater was energized to the heat flux levels corresponding to those of the falling film tests and the thermocouples were calibrated for the offset caused by passing d.c. current

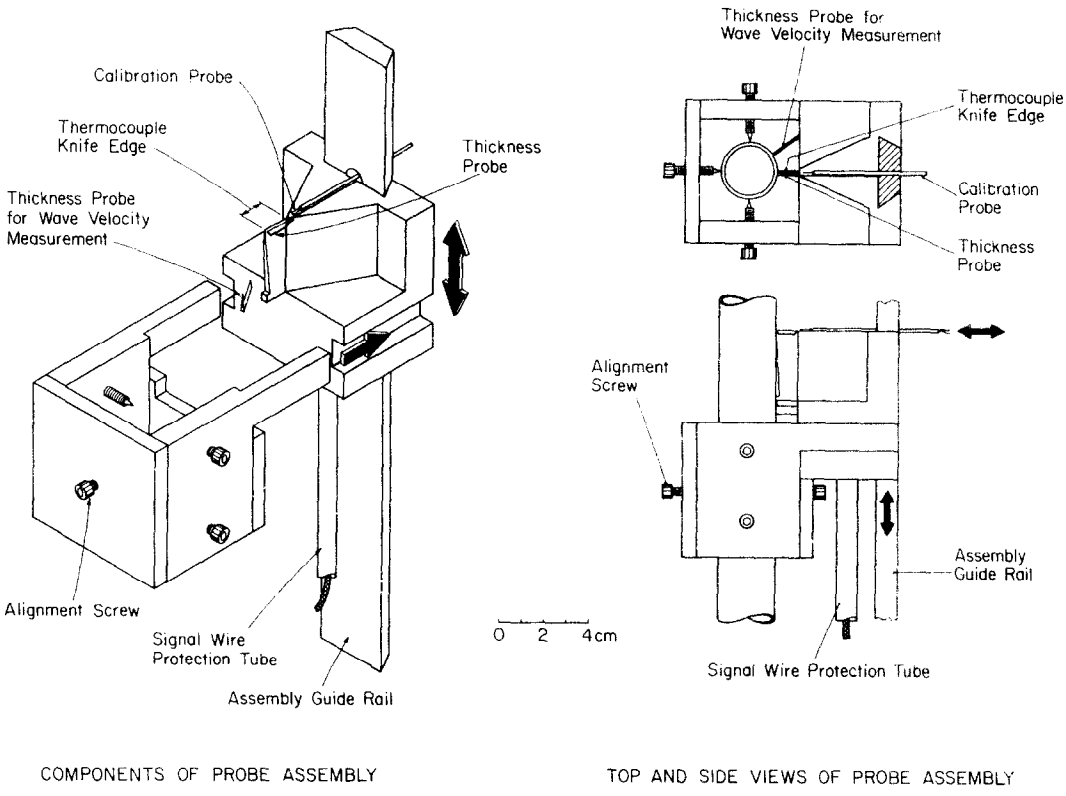

FIG. 3. Probe assembly.

through the heater. Calibration of this voltage offset was repeated several times after using the same batch of deionized water in the falling film configuration. A testing period of 4 h was established as an upper limit for using the same water in order to maintain thermocouple offset below 0.2°C. Longer testing periods were found to produce higher offset values due to very fine particles entraining with the water during prolonged circulation in the loop.

The inside wall temperature was measured at 17 locations by type-T (copper–constantan) thermocouple pairs made from 0.127 mm diameter wire. Thermocouples in each pair were oriented 180 deg apart in the circumferential direction, allowing for vertical alignment of the test section to ensure a symmetrical falling film during each experiment. A maximum temperature difference of 0.1°C between two thermocouples at the same vertical location was accepted as a condition of evenly distributed film flow. The inner thermocouple assembly was described in detail in ref. [1].

Among the techniques available for film thickness measurement, the parallel wire electrical conductance probe was reported as a method for accurate measurement of instantaneous film thickness by Miya *et al.* [18], Brown *et al.* [21], Karapantsios *et al.* [22] and Koskie *et al.* [23]. However, the need to dissolve an electrolyte in the film precluded this technique for direct contact resistive heating of deionized water. Therefore, an alternate technique based upon the principle of hot-wire anemometry was developed for the present study. The thickness probe was made from 0.0254 mm diameter platinum–10% rhodium wire, Fig. 5, which was stretched across the liquid–gas interface. A constant d.c. current was applied through the probe wire, and film thickness was determined from variations in the probe voltage drop.

The film thickness measurement technique is based upon two important features. One is the large ratio of heat transfer coefficient over the probe wire in the liquid to that in the gas. The other is the strong relationship between electrical resistance and temperature for some electrically conducting materials. By applying a constant current through the probe, the voltage signal becomes a function of thickness because the total electrical resistance depends on the length of wire in the liquid. Choosing a wire material having high resistivity and a relatively large temperature coefficient of resistivity enhances voltage signal sensitivity to film thickness fluctuation.

Calibration of the thickness probe was achieved in several ways. First, the probe was submerged vertically downward into a small test cell containing a stagnant layer of water. A plot of probe voltage output vs water layer thickness confirmed the probe performance was highly linear. *In situ* calibration was also performed prior to each test at heating conditions identical to those of the test itself using the calibration probe shown in Fig. 5. While the thickness probe was mounted across the film, the calibration probe was

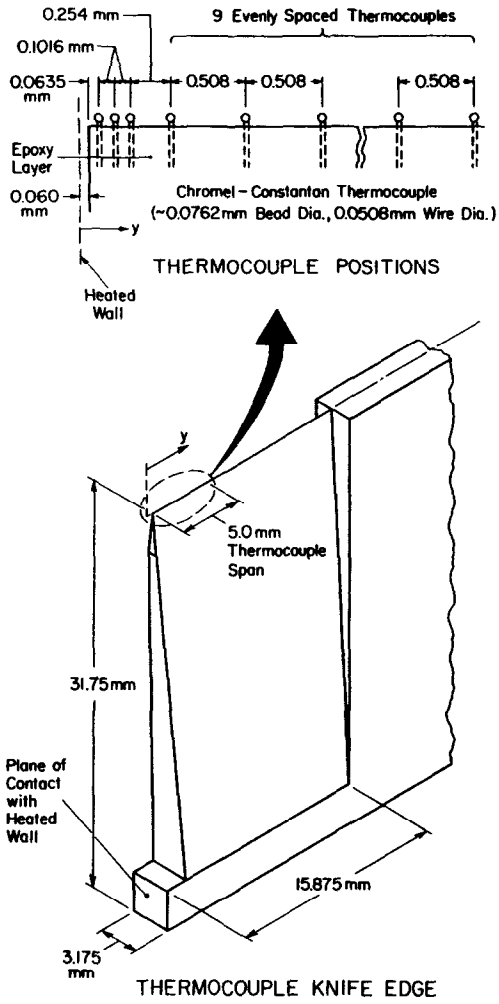

FIG. 4. Thermocouple positions on the thermocouple knife edge. Actual positions deviate slightly from the values shown. The actual positions cited in Section 3 of this paper were measured under the microscope.

translated horizontally towards the film interface. Contact between the tip of the calibration probe and the film interface triggered surges in the calibration probe signal. The contact time was recorded in order to identify the corresponding voltage signal of the thickness probe, providing a single calibration point. This calibration was repeated by translating the calibration probe to new positions closer to the heated wall. The measurement resolution and response time of the thickness probe were determined to be 0.05 mm and 0.14 ms, respectively. Other details concerning the construction and transient characteristics of the thickness probe can be found elsewhere [24].

Data were collected by a high speed Keithley Series 500 data acquisition and control system interfaced with a Compaq Deskpro 386 Model 40 microcomputer. Temperature profile data (up to 12 signals) were obtained across the film along with the thickness data over a sampling period of 1 s with a sampling frequency of 500 Hz. Data for the statistical analysis (one temperature signal along with the thickness signal), such as correlations and spectral studies, were taken with a sampling frequency of 400 Hz rather than 500 Hz to increase the sampling period from 4 to 5 s. The sampling frequency of 400 Hz is much higher than typical maximum dominant frequencies ($\sim$20 Hz) of film thickness. The temperature data were processed by low pass filtering the time records using a fourth order, 0.1 dB Chebyshev digital filter code written by Walraven [25]. A low pass filter cutoff frequency of 100 Hz was used for filtering external noise with negligible influence on the temperature data.

3. EXPERIMENTAL RESULTS

Experiments were performed with water over a film Reynolds number between 2700 and 11 700 and heat flux ranging from 0 to 75 000 W m^{-2}. Figures 6(a) and (b) show time records of liquid temperature measured simultaneously at five distances from the wall along with the corresponding thickness record. Durations of intermittent exposure of thermocouples to the gas side increase monotonically with increasing thermocouple distance from the wall. This is shown in Figs. 6(a) and (b) in the form of discontinuities in some temperature records especially for the thermocouples further from the wall. These discontinuities were programmed as acquisition time bands for temperature data corresponding to instantaneous values of thickness smaller than the thermocouple-to-wall distance. All the data in the present study showed a liquid temperature variation relatively opposite to the variation of film thickness. The liquid temperature increased in the thin, low thermal mass portions of the film and decreased in the large waves which carry a relatively large thermal mass of liquid. Figure 6(a) also shows that the relationship between temperature and thickness is fairly consistent across the entire film thickness.

The general trend of the relationship between temperature and thickness shown in Fig. 6(a) is consistent with trends reported by Ganchev and Trishin [20] on heat transfer to a wavy film. For the range of Reynolds numbers tested, the effect of interfacial waves on liquid temperature was most significant for $Re \leqslant 5000$ and less noticeable for $Re \geqslant 10\,000$, even at heat fluxes as high as 50 000 W m^{-2} as shown in Fig. 6(b). The temperature fluctuation for a given Reynolds number increased monotonically as heat flux was increased to steady-state values between 0 and 75 000 W m^{-2}. Two reasons can be suggested to explain the relative insensitivity of thickness to heat flux at high Reynolds numbers. First, since the film substrate between large waves increases in thickness, thermal mass and velocity with increasing Reynolds number, wave-induced temperature changes are expected to dampen at high Reynolds numbers compared to lower Reynolds numbers. Second, the temperature changes become weaker

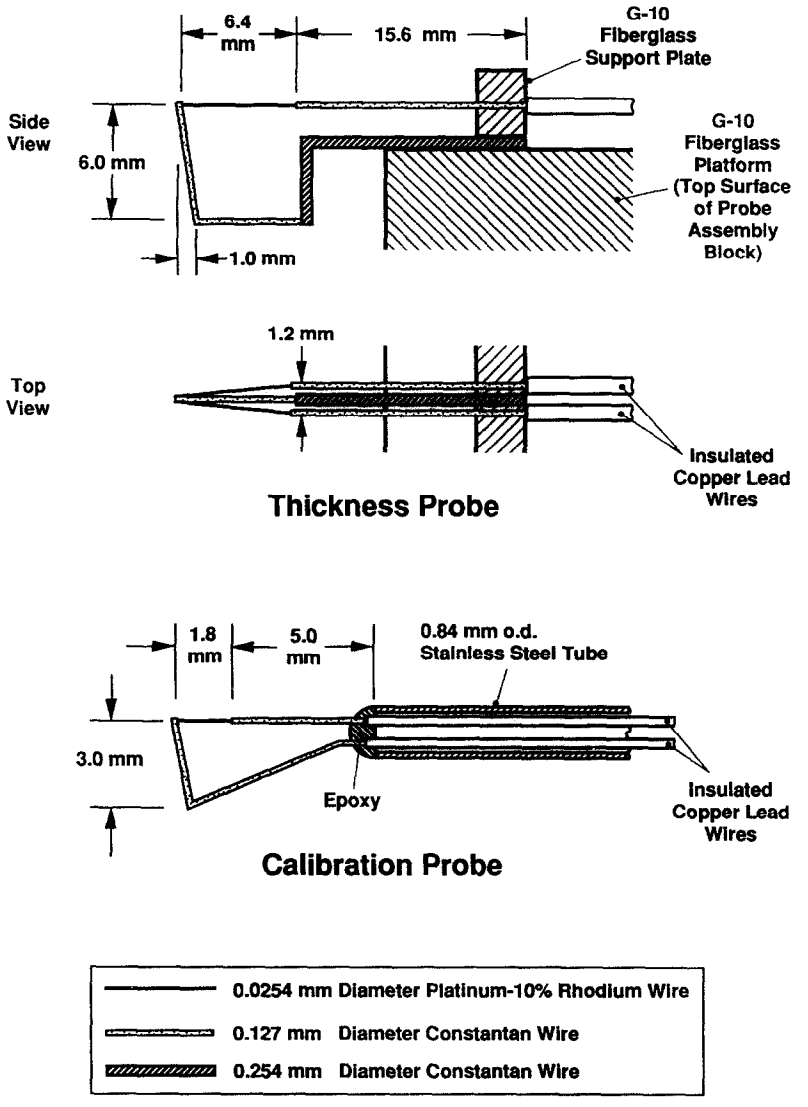

FIG. 5. Schematic diagrams of the thickness probe and thickness calibration probe.

at high Reynolds numbers due to a stronger intensity of turbulence mixing.

Figure 7 shows thermocouple distances from the wall nondimensionalized with respect to film thickness plotted against liquid temperature nondimensionalized with respect to the difference between the wall and interface temperatures. Clearly displayed are marked differences between the temperature profile within the large wave from those in the upstream and downstream substrate regions. Figure 7 also shows some periodicity in the temperature profile associated with large wave motion past the measurement location.

Figures 8(a) and (b) show composite plots of measured liquid temperature, thermocouple location and time. The temperature data shown were interpolated using a cubic spline fit described by Gerald and Wheatley [26]. The diminishing influence of waviness on liquid temperature with increasing Reynolds number is clearly manifested in comparing the two plots. Figures 8(a) and (b) show occasional excursion of temperature to high values within the relatively cool liquid in the large wave. This phenomenon can be attributed to fluid circulation in the wave as proposed by many investigators [27–30]. Numerical results by Maron *et al.* [15], and Wasden and Dukler [16, 17] show that the interation between a large wave and a thin substrate causes an acceleration of fluid from the upstream substrate toward the crest of the large wave. Hence, high temperature liquid from the substrate can be transported to the cold region within the large wave before losing its excess thermal energy due to full mixing. The temperature excursion phenomenon is represented in Fig. 9. The flow streamlines are drawn with respect to a wall moving at a velocity equal to the wave velocity, V_w. These streamlines are qualitatively based on the numerical results of previous investigators [15, 16].

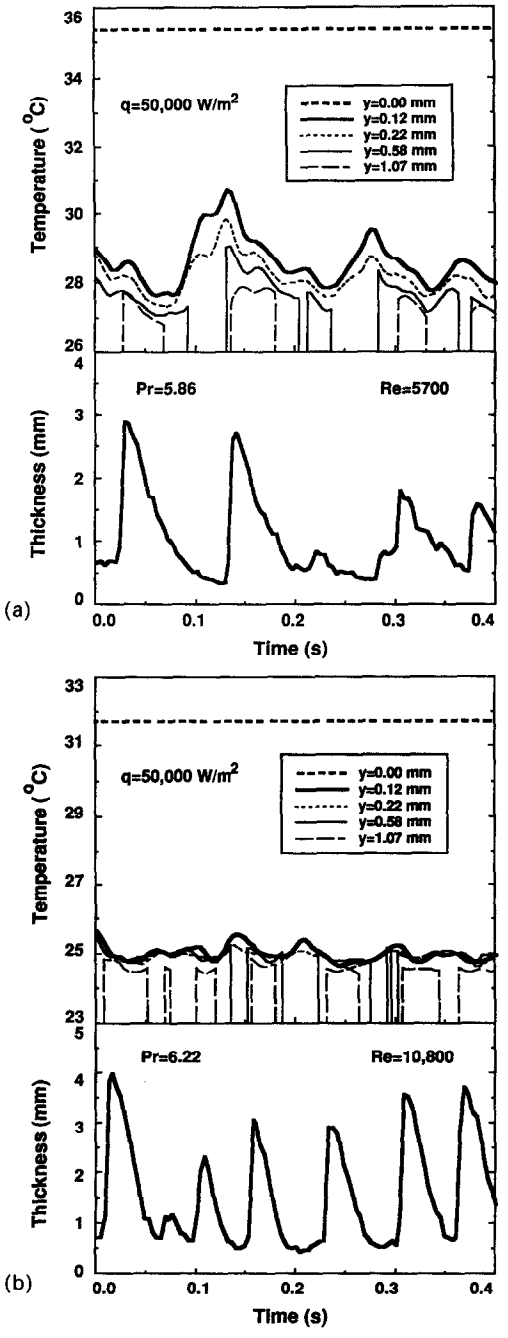

FIG. 6. Time records of film thickness and liquid temperature for: (a) $Re = 5700$; (b) $Re = 10\,800$.

Figure 9 shows how temperature measured at a fixed location from the wall undergoes excursions within the wave which are superimposed on the overall trends of increasing mean temperature of the liquid in the flow direction and the periodic cooling effect of large waves.

It should be noted that the relationship between liquid temperature and thickness is complicated by the randomness of fluid flow due to interaction between small waves or ripples and the large waves as well as between adjacent large waves. The renewal–penetration hypothesis of turbulence [31, 32] may also explain some of the hot and cold temperature excursions displayed in Figs. 8(a) and (b). Based on this hypothesis, it may be postulated that some random turbulent eddies from the low temperature core of the large wave intermittently penetrate much closer to the wall than other eddies do. Accordingly, heat transfer in some regions near the wall may undergo excursions of unsteady molecular diffusion due to the cold eddies.

4. STATISTICAL ANALYSIS

4.1. *Statistical parameters*

The measured time records of film thickness, $\delta(t)$, and liquid temperature at $y = 0.12$ mm, $T(t)$, were treated as random or stochastic variables. The time records were examined with the aid of statistical tools based on the assumption that the two variables are stationary and ergodic in nature. While the various statistical functions describing two variables are time-invariant based on the premise of stationarity, time averages are equated with ensemble averages under the postulation of ergodicity.

Time series analysis was employed to obtain statistical parameters of a random variable, $s(t)$, which represents film thickness, $\delta(t)$, or liquid temperature, $T(t)$, such as probability distribution, $P(s)$, probability density, $p(s)$, mean, $\bar{s}$, variance (second moment about the mean), σ^2, autocovariance, $R(\tau)$, and autospectrum, $S(f)$. For a data record of N samples, these statistical parameters can be defined as follows [33, 34]:

$$P(s) = \text{Prob}\,[s(t) < s] = \frac{n\{s(t) < s\}}{N} \tag{1}$$

$$p(s) = \lim_{\Delta s \to 0} \frac{\text{Prob}\,[s < s(t) < s + \Delta s]}{\Delta s} = \frac{\mathrm{d}P(s)}{\mathrm{d}s} \tag{2}$$

$$\bar{s} = \int_{-\infty}^{\infty} s(t)p(s)\,\mathrm{d}s = \frac{1}{N}\sum_{i=1}^{N} s_i(t) \tag{3}$$

$$\sigma^2 = \int_{-\infty}^{\infty} [s(t) - \bar{s}]^2 p(s)\,\mathrm{d}s = \frac{1}{N}\sum_{i=1}^{N} [s_i(t) - \bar{s}]^2 \tag{4}$$

$$R(\tau) = \lim_{\tau_s \to \infty} \frac{1}{\tau_s \sigma^2} \int_0^{\tau_s} [s(t) - \bar{s}][s(t+\tau) - \bar{s}]\,\mathrm{d}t$$

$$= \frac{1}{N\sigma^2} \sum_{i=1}^{N} [s(t) - \bar{s}][s(t+\tau) - \bar{s}] \tag{5}$$

$$S(f) = \int_{-\infty}^{\infty} R(\tau)\, \mathrm{e}^{-j2\pi f\tau}\,\mathrm{d}\tau \tag{6}$$

where n is the number of samples in a subset of the data record. The cross-covariance, $C(\tau)$, and cross-spectrum, $W(f)$, between film thickness and liquid temperature are defined as

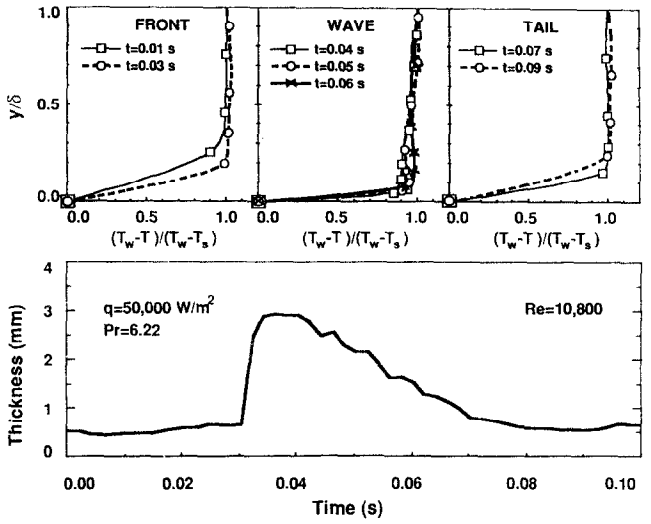

FIG. 7. Temperature profiles at different times within a wave period.

$$C_{12}(\tau) = \lim_{\tau_s \to \infty} \frac{1}{\tau_s \sigma_1 \sigma_2} \int_0^{\tau_s} [s_1(t) - \bar{s}_1][s_2(t+\tau) - \bar{s}_2]\,\mathrm{d}t$$

$$= \frac{1}{N\sigma_1\sigma_2} \sum_{t=1}^{N} [s_1(t) - \bar{s}_1][s_2(t+\tau) - \bar{s}_2] \quad (7)$$

$$W_{12}(f) = \int_{-\infty}^{\infty} C_{12}(\tau)\, \mathrm{e}^{-i2\pi f\tau}\,\mathrm{d}\tau \quad (8)$$

where subscripts '1' and '2' represent film thickness and liquid temperature, respectively. In the remainder of this paper a *data set* utilized in evaluating a given statistical parameter is defined as having a total of 2000 samples obtained at a frequency of 400 Hz.

4.2. *Statistical results*

Figure 10 shows probability density distributions of film thickness for the range $3000 \leqslant Re \leqslant 11\,700$ corresponding to four heat fluxes. Each curve is a mean of distributions measured for eight data sets at identical operating conditions. The distributions show much concentration of thickness data in the lower thickness range and a wider, less concentrated distribution over higher thickness values. The lower Reynolds numbers show a more severe concentration around $\delta = 0.5$ mm, while the higher Reynolds number distributions show less concentration around values well above 0.5 mm. The relatively high probability density corresponding to small thickness values for $Re = 3000$–3200 is a manifestation of a near-zero substrate thickness between large waves. For $Re = 10\,000$–$11\,700$, on the other hand, there exists a more continuous substrate having a minimum thickness slightly smaller than 0.5 mm. The present probability density distributions of thickness are consistent with those by Karapantsios *et al.* [22] who suggested a Weibull distribution for adiabatic films in the range $509 \leqslant Re \leqslant 9000$ and a log-normal distribution in the range $9000 \leqslant Re \leqslant 13\,090$.

The lower Reynolds number range in Fig. 10 also shows sensitivity to heat flux compared to a distribution rather invariant with heat flux for $Re \geqslant 5000$. Heat flux is expected to affect thickness in many ways. For a fixed flow rate, increasing the flux raises liquid temperature, resulting in a lower kinematic viscosity and, consequently, a higher Reynolds number. Heating could also affect the hydrodynamic structure of the interfacial waves due to the reduced kinematic viscosity and surface tension and due to the surface tension temperature gradients. This is shown in Fig. 10 for $Re = 3000$–3200 by a slight reduction in probability density for $\delta \approx 0.5$ mm and a slight increase for the higher film thickness associated with large waves.

Figure 11 shows the effect of heat flux on film thickness variance nondimensionalized with respect to the variance at zero heat flux. At Reynolds numbers in the range $2700 \leqslant Re \leqslant 3200$ the variance increases monotonically with increasing heat flux. This trend may be explained by the effects of thermocapillary forces on fluid motion in heated films. As shown in Fig. 10, the substrate region between large waves becomes very thin for $Re = 2700$–3200. Thus, the film is expected to undergo a relatively large temperature rise in the thin regions, becoming hotter than the large waves as shown previously in Figs. 6(a) and 8(a). The surface tension force becomes stronger at the interface of the large wave and weaker at the substrate interface. The larger force tends to pull liquid away from the thin substrate toward the large wave, resulting in an increased variance of film thickness. This force becomes weaker at higher Reynolds numbers where the substrate is relatively thick and less prone to excessive temperature rise as was indeed shown in Figs. 6(b) and 8(b). This might explain the relative insensitivity of thickness variance to heat flux at high fluxes, but it does not explain the peak values of variance shown in Fig. 11 for Reynolds numbers exceeding 3200.

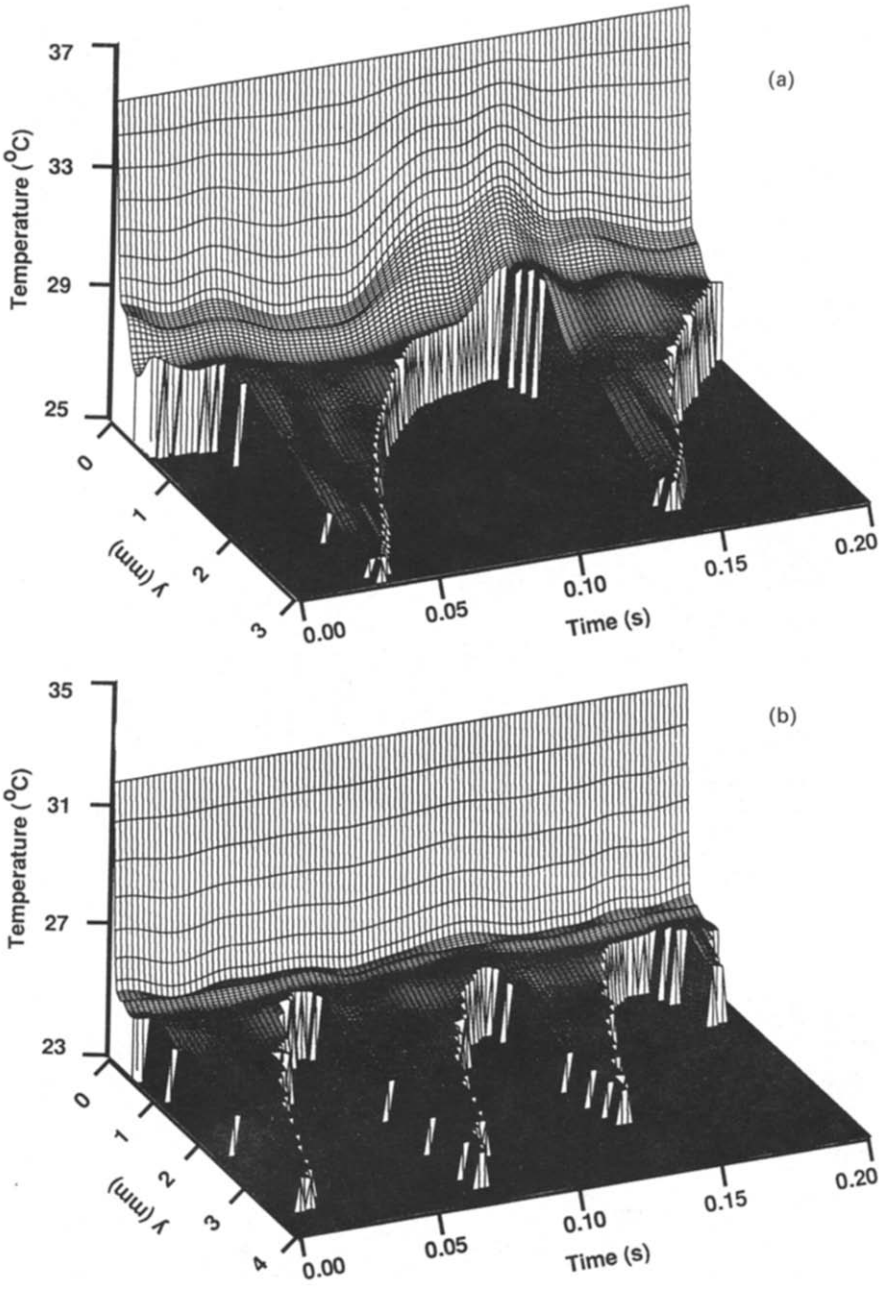

FIG. 8. Three-dimensional plots of liquid temperature variation at various distances from the wall with time for: (a) $Re = 5700$; (b) $Re = 10\,800$.

Figure 12 shows probability density distribution for the liquid temperature averaged from eight data sets obtained at identical operating conditions. As expected, increasing the heat flux increases the magnitude of the temperature gradient across the film and widens the temperature band. Most noticeable is the wide distribution of liquid temperature, 0–13°C, for $Re = 3000$–3200 at $q = 75\,000$ W m^{-2} compared to a very concentrated distribution, 0–0.7°C, for the other extreme condition corresponding to $Re = 10\,000$–$11\,700$ and $q = 10\,000$ W m^{-2}. This is the reason why different temperature scales were chosen in plotting the probability density distributions in Fig. 12 corresponding to the different Reynolds number ranges. These results are consistent with the high and low temperature fluctuations between the substrate and large wave regions discussed earlier in conjunction with Figs. 8(a) and (b). The probability density of liquid temperature shown in Fig. 12 exhibits a Gumbel type distribution [35], yet most results can be fitted with small error for the ranges $Re \geqslant 10\,000$ and $q \leqslant 75\,000$ W m^{-2} using a normal Gaussian distribution.

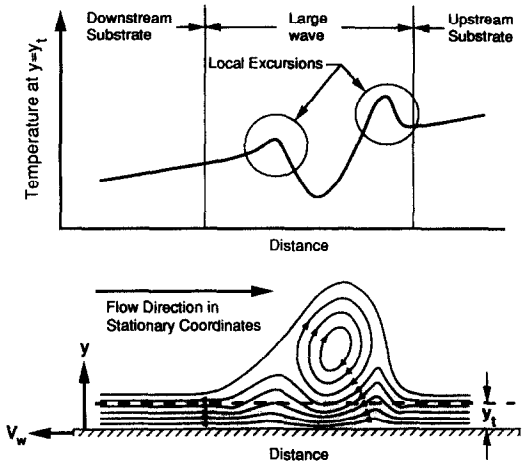

FIG. 9. Qualitative representation of liquid temperature variation within a large wave at a fixed distance from the wall.

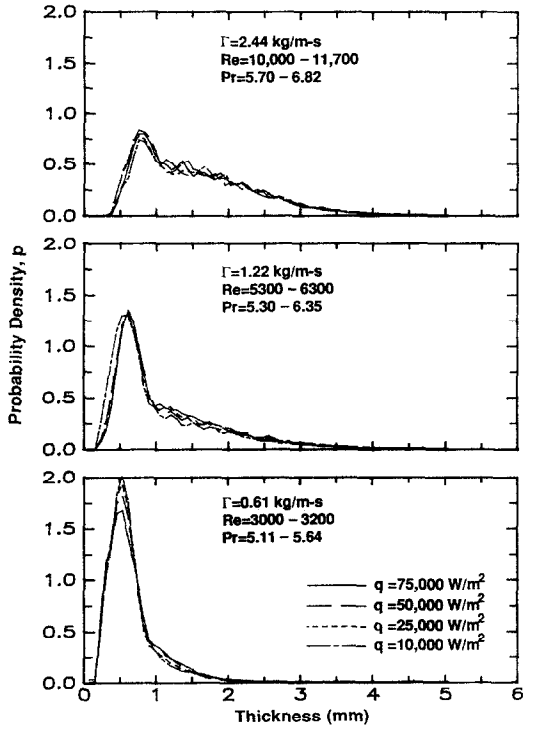

FIG. 10. Probability density of film thickness at different flow rates and heat fluxes.

Figures 13(a) and (b) show autocovariance functions calculated for film thickness and liquid temperature, and cross-covariance between the two parameters. The results shown are averages of values calculated from four data sets. The autocovariance plots of Fig. 13(a) show repeatability in wave shape corresponding to a period (time lag) of approximately 0.1 s compared to a weaker repeatability for temperature. However, there seems to be a strong relationship between waviness and temperature as indicated by the first absolute peak on the cross-correlation plot. The cross-correlation plot, Fig. 13(a),

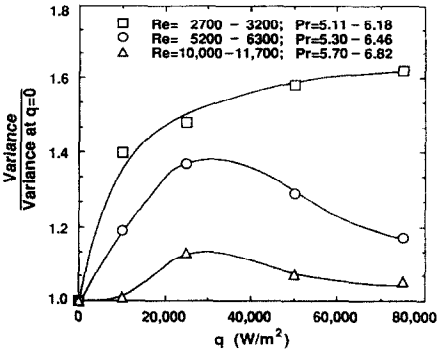

FIG. 11. Nondimensionalized variance of film thickness with increasing heat flux.

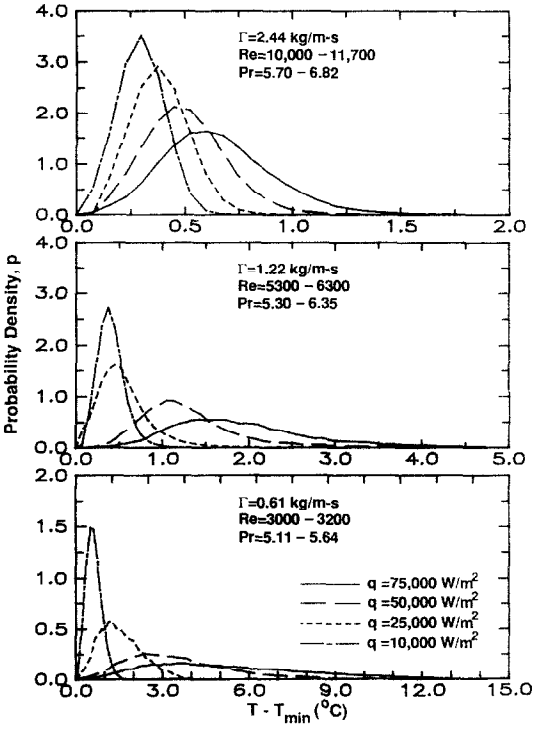

FIG. 12. Probability density of liquid temperature at different flow rates and heat fluxes.

shows the variations of the two parameters are not exactly opposite since the first absolute peak value does not correspond to a zero time lag. The 'phase shift' between the two signals suggests temperature reaches its lowest value within a large wave shortly after thickness attains its maximum (wave crest) value as was clearly pointed out in the previous section of this paper and illustrated in Fig. 9.

Increasing heat flux enhanced the relationship between thickness and temperature as displayed by the increasing amplitude of the first absolute peak value of the cross-covariance function. By comparing Figs. 13(a) and (b) it becomes apparent that higher Reynolds numbers require a greater heat flux to initiate a strong correlation between the two signals. The correlation is virtually nonexistent at $Re =$

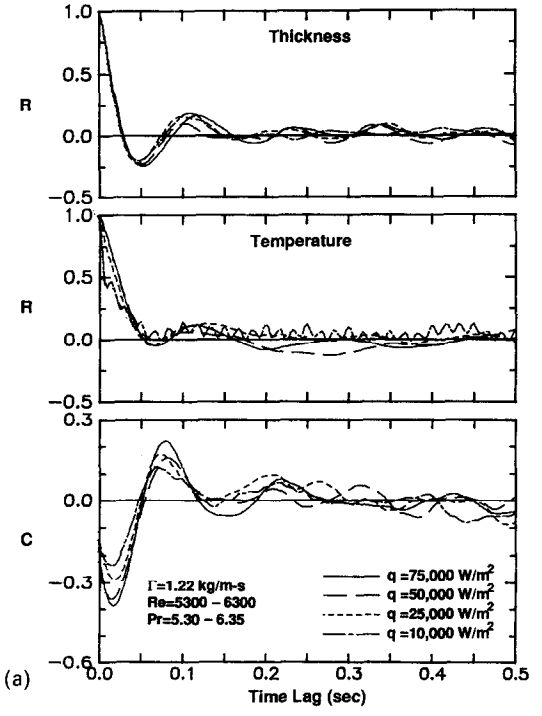

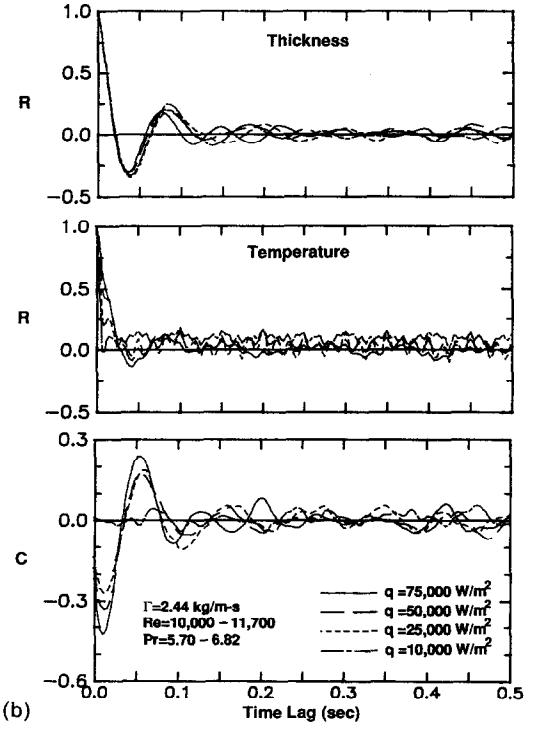

FIG. 13. Autocovariance and cross-covariance results for: (a) Re = 5300–6300; (b) Re = 10 000–11 700.

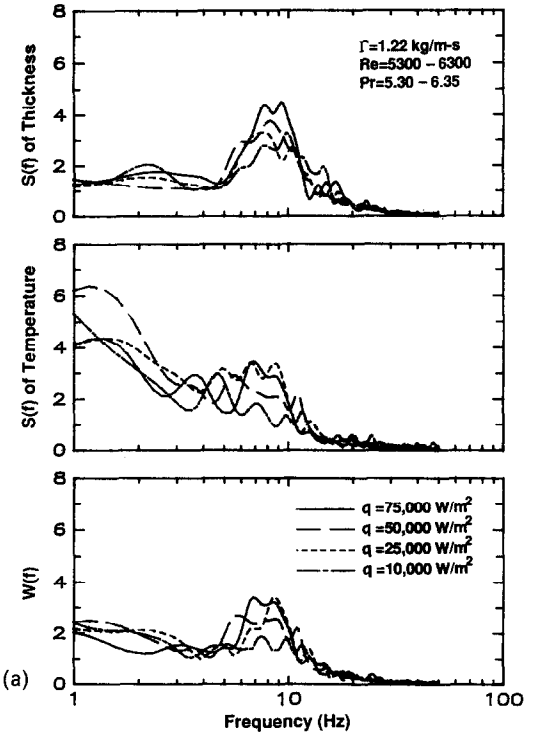

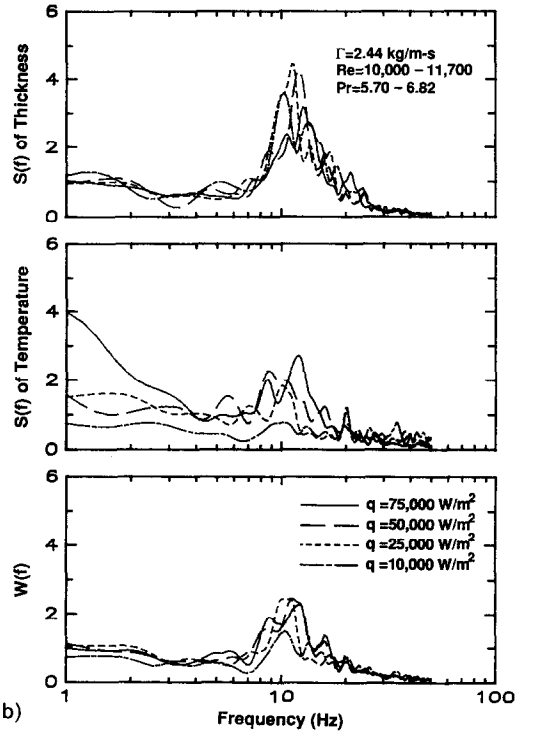

FIG. 14. Autospectrum and cross-spectrum results for: (a) Re = 5300–6300; (b) Re = 10 000–11 700.

10 000–11 7070 and a relatively low heat flux of 10 000 W m^{-2}. It should be noted that some signal noise is prevalent in the autocovariance function of temperature for some relatively low heat flux levels as shown in Figs. 13(a) and (b).

Figures 14(a) and (b) show autospectra of film thickness and liquid temperature and cross-spectra of the two signals. Following a method previously employed by Karapantsios *et al.* [22] in analyzing adiabatic film thickness data, the present spectra were calculated using the first three groups (segments) of 512 (=2^9) samples from each data set of 2000

samples. To improve frequency resolution, each segment was analyzed independently by using the measured values in the range 1–512 and assigning zero values to the sample sequence 513–2048 ($=2^{11}$). Then a Hanning window function was applied to reduce side-lobe leakage [33]. Spectral results were calculated for each segment using a Fast Fourier Transform (FFT) code written by Newland [34] and averaged for the three segments in a single data base. Representative spectra were finally obtained by averaging results from four data bases obtained at identical operating conditions. The error band in this spectral averaging technique is 14% [22, 23]. Figures 14(a) and (b) show representative autospectra normalized by the variance of the individual variable and cross-spectra normalized by the square root of the product of the two variances. Film thickness shows a dominant frequency band with peak autospectrum values ranging from 5 to 11 Hz as Re is increased from 3000 to 11 700. This trend of increasing dominant frequencies in the autospectrum of film thickness with increasing Reynolds number was also reported by Chu and Dukler [36]. A similar trend is also shown in the temperature autospectrum within the dominant frequency range of the corresponding thickness autospectrum. However, the temperature autospectrum is not as concentrated. The cross-spectra show distinct bands of dominant frequencies similar to those of the corresponding thickness autospectra. The dominant band shifts to higher frequencies with increasing Reynolds number.

5. CONCLUSIONS

Simultaneous measurements of instantaneous liquid temperature in a falling film and film thickness were examined qualitatively and analyzed statistically to investigate the relationship between interfacial waves and heat transfer to the film. Key conclusions from the study are as follows:

(1) Liquid temperature at a fixed distance from the wall generally increases in the thin substrate portions of the film and decreases within the large waves.

(2) The effect of waviness on temperature becomes insignificant for film Reynolds numbers greater than 10 000 and wall heat fluxes less than approximately 50 000 W m^{-2}.

(3) Liquid temperature undergoes periodic changes with the passage of a large wave. The temperature profile within the large wave is markedly different from those in the substrate upstream and downstream of the large wave.

(4) Local excursions in temperature modify the general transient cooling effect of large waves. These excursions may be attributed to acceleration of hot liquid from the upstream substrate as it mixes with the cool fluid of the large wave. The excursions may also be the results of interaction between adjacent waves or the random penetration of cool eddies close to the wall.

(5) The effect of increasing heat flux on probability density and variance of film thickness was stronger at low Reynolds numbers compared to high Reynolds numbers. Since films having low Reynolds numbers acquire near-zero substrate thickness between the large waves, it is suggested that the relatively large temperature rise in the substrate regions can induce large changes in liquid properties and corresponding changes in the hydrodynamic structure of the film. For example, the surface tension force becomes stronger at the interface of the large wave and weaker at the substrate interface. The resultant force tends to pull liquid away from the thin substrate toward the large wave, increasing the variance of film thickness. These property changes become less significant at higher Reynolds numbers due to a thickening in substrate thickness and a dampening of temperature rise in the substrate.

(6) Cross-covariance between thickness and temperature increases with increasing heat flux and points to variations in two variables which are not exactly opposite but having a slight 'phase shift' due to temperature excursions associated with relative liquid motion between the substrate and the large wave.

(7) Cross-spectrum between thickness and temperature shows a distinct band of dominant frequencies in the relationship between the two variables. Increasing the film Reynolds number shifts the band to higher frequencies.

Acknowledgement—This paper is based upon work supported by the U.S. Department of Energy, Office of Basic Energy Sciences through Grant No. DE-85ER133398.

REFERENCES

1. J. A. Shmerler and I. Mudawar, Local heat transfer coefficient in wavy free-falling turbulent liquid films undergoing uniform sensible heating, *Int. J. Heat Mass Transfer* **31**, 67–77 (1988).
2. J. A. Shmerler and I. Mudawar, Local evaporative heat transfer coefficient in turbulent free-falling liquid films, *Int. J. Heat Mass Transfer* **31**, 731–742 (1988).
3. P. L. Kapitza, *Collected Papers of P. L. Kapitza*, Vol. II. Pergamon Press, New York (1965).
4. T. B. Benjamin, Wave formation in laminar flow down an inclined plane, *J. Fluid Mech.* **2**, 554–574 (1957).
5. A. M. Binnie, Experiments on the onset of wave formation on a film of water flowing down a vertical plane, *J. Fluid Mech.* **2**, 551–553 (1957).
6. C. S. Yih, Stability of liquid flow down an inclined plane, *Physics Fluids* **6**(3), 321–334 (1963).
7. S. V. Alekseenko, V. E. Nakoryakov and B. G. Pokusaev, Wave formation on vertical falling liquid films, *Int. J. Multiphase Flow* **11**, 607–627 (1985).
8. N. Brauner, D. M. Maron and W. Zijl, Interfacial collocation equations of thin liquid film: stability analysis, *Chem. Engng Sci.* **42**, 2025–2035 (1987).
9. H. C. Chang, Evolution of nonlinear waves on vertically falling films—a normal form analysis, *Chem. Engng Sci.* **42**, 515–533 (1987).
10. K. R. Chun and R. A. Seban, Heat transfer to evaporating liquid films, *J. Heat Transfer* **93**, 391–396 (1971).

11. R. A. Seban and A. Faghri, Evaporation and heating with turbulent falling liquid films, *J. Heat Transfer* **98,** 315–318 (1976).
12. G. J. Gimbutis, A. J. Drobavicius and S. S. Sinkunas, Heat transfer of a turbulent water film at different initial flow conditions and high temperature gradients, *Proc. 6th Int. Heat Transfer Conf.*, Toronto, Canada, Vol. 1, pp. 321–326 (1978).
13. S. M. Yih and J. L. Liu, Prediction of heat transfer in turbulent falling films with or without interfacial shear, *A.I.Ch.E. Jl* **29,** 903–909 (1983).
14. I. Mudawar and M. A. El-Masri, Momentum and heat transfer across freely-falling turbulent liquid films, *Int. J. Multiphase Flow* **12,** 771–790 (1986).
15. D. M. Maron, N. Brauner and G. F. Hewitt, Flow patterns in wavy thin films: numerical simulation, *Int. Commun. Heat Mass Transfer* **16,** 655–666 (1989).
16. F. K. Wasden and A. E. Dukler, Insights into the hydrodynamics of free falling wavy films, *A.I.Ch.E. Jl* **35,** 187–195 (1989).
17. F. K. Wasden and A. E. Dukler, Numerical investigation of large wave interactions on free falling films, *Int. J. Multiphase Flow* **15,** 357–370 (1989).
18. M. Miya, D. Woodmansee and T. J. Hanratty, A model for roll waves in gas–liquid flow, *Chem. Engng Sci.* **26,** 1915–1931 (1971).
19. N. Brauner and D. M. Maron, Characteristics of inclined thin films, waviness and the associated mass transfer, *Int. J. Heat Mass Transfer* **25,** 99–110 (1982).
20. B. G. Ganchev and V. V. Trishin, Fluctuation of wall temperature in film cooling, *Fluid Mech.—Sov. Res.* **16,** 17–23 (1987).
21. R. C. Brown, P. Andreussi and S. Zanelli, The use of wire probes for the measurement of liquid film thickness in annular gas–liquid flows, *Can. J. Chem. Engng* **56,** 754–757 (1978).
22. T. D. Karapantsios, S. V. Paras and A. J. Karabelas, Statistical characteristics of free falling films at high Reynolds numbers, *Int. J. Multiphase Flow* **15,** 1–21 (1989).
23. J. E. Koskie, I. Mudawar and W. G. Tiederman, Parallel-wire probes for measurement of thick liquid films, *Int. J. Multiphase Flow* **15,** 521–530 (1989).
24. T. H. Lyu, Interfacial wave effects on heat transfer to a falling liquid film, Ph.D. Thesis, Purdue University, West Lafayette, Indiana (1990).
25. R. Walraven, Digital filters, *Proc. Digital Equipment Computer Users Society*, San Diego, California, pp. 827–834 (1980).
26. C. F. Gerald and P. O. Wheatley, *Applied Numerical Analysis*, 3rd Edn. Addison-Wesley, Reading, Massachusetts (1985).
27. S. Portalski, Eddy formation in film flow down a vertical plate, *I&EC Fundam.* **3,** 49–53 (1964).
28. F. P. Stainthorp and G. J. Wild, Film flow—the simultaneous measurement of wave amplitude and the local mean concentration of a transferrable component, *Chem. Engng Sci.* **22,** 701–704 (1967).
29. A. E. Dukler, The roll of waves in two phase flow: some new understandings, *Chem. Engng Educ. 1976 Award Lecture*, pp. 108–138 (1977).
30. N. Brauner and D. M. Maron, Modelling of wavy flow in inclined thin film, *Chem. Engng Sci.* **38,** 775–788 (1983).
31. P. V. Danckwerts, Significance of liquid-film coefficients in gas absorption, *Ind. Engng Chem.* **43,** 1460–1467 (1951).
32. L. C. Burmeister, *Convective Heat Transfer*. Wiley, New York (1983).
33. J. S. Bendat and A. G. Piersol, *Engineering Applications of Correlation and Spectral Analysis*. Wiley, New York (1980).
34. D. E. Newland, *An Introduction to Random Vibrations and Spectral Analysis*, 2nd Edn. Longman, New York (1984).
35. E. Castillo, *Extreme Value Theory in Engineering*. Academic Press, San Diego, California (1988).
36. K. J. Chu and A. E. Dukler, Statistical characteristics of thin, wavy films, part III. Structure of the large waves and their resistance to gas flow, *A.I.Ch.E. Jl* **21,** 583–593 (1975).

ETUDE STATISTIQUE DE LA RELATION ENTRE L'ONDULATION DE L'INTERFACE ET LE TRANSFERT THERMIQUE PAR CHALEUR SENSIBLE POUR UN FILM LIQUIDE TOMBANT

Résumé—Des expériences sont conduites pour éclairer les aspects du transfert thermique d'un film liquide avec ondulations. L'épaisseur locale du film et la température du liquide sont mesurées simultanément en utilisant une sonde d'épaisseur à conductance thermique et des thermocouples à réponse rapide, le film s'écoulant sur une paroi chauffée électriquement. La température du liquide à une distance fixe de la paroi croît généralement dans la mince zone pariétale du film et décroît dans les grandes ondes. Les excursions de température sont compliquées dans les grandes ondes à cause des tourbillons turbulents et du mouvement relatif de liquide entre l'onde et le substrat environnant. Les mesures sont examinées à l'aide des outils statistiques pour étudier la relation entre l'épaisseur du film et la température du liquide à différents nombres de Reynolds de film et flux thermiques. La corrélation entre les deux variables est plus forte aux grands qu'aux faibles flux. Une analyse spectrale montre une bande distincte de fréquences dominantes dans la relation entre les deux variables.

STATISTISCHE UNTERSUCHUNG DES ZUSAMMENHANGS ZWISCHEN DER OBERFLÄCHENWELLIGKEIT UND DEM TRANSPORT FÜHLBARER WÄRME AN EINEN RIESELFILM

Zusammenfassung—Um einen Einblick in die Mechanismen des Wärmetransports an einen welligen Rieselfilm zu erhalten, werden Experimente durchgeführt. Die örtliche Dicke und die Temperatur eines welligen Films, der entlang einer elektrisch beheizten Wand abläuft, werden gleichzeitig mit Hilfe einer Wärmeleitungssonde bzw. schnell ansprechender Thermoelemente gemessen. Die Temperatur der Flüssigkeit in einem bestimmten Abstand von der Wand wächst grundsätzlich in der dünnen Unterschicht des Films an und fällt dann im Bereich der großen Wellen ab. Die Temperatur zeigt im Bereich der großen Wellen aufgrund der turbulenten Wirbel und der Relativbewegung der Flüssigkeit zwischen den großen Wellen und deren Umgebung ein kompliziertes Verhalten. Um den Zusammenhang zwischen Filmdicke und Flüssigkeitstemperatur bei verschiedenen Reynolds-Zahlen und Wärmestromdichten zu untersuchen, werden die Messungen mit Hilfe statistischer Hilfsmittel geprüft. Bei großen Wärmestromdichten korrelieren die beiden Variablen stärker als bei kleinen Wärmestromdichten. Die Kreuzkorrelation zeigt ein ausgeprägtes Band vorherrschender Frequenzen im Verhältnis der beiden Variablen zueinander.

СТАТИСТИЧЕСКОЕ ИССЛЕДОВАНИЕ ВЗАИМОСВЯЗИ МЕЖДУ ВОЛНИСТОСТЬЮ ГРАНИЦЫ РАЗДЕЛА И МАССОПЕРЕНОСОМ К СТЕКАЮЩЕЙ ЖИДКОЙ ПЛЕНКЕ

Аннотация—Экспериментально исследуются характеристики теплопереноса при стекании волнистой жидкой пленки. Проводится измерение локальных толщины пленки и температуры жидкости с использованием датчика и малоинерционной термопары в процессе стекания волнистой пленки вдоль нагреваемой электрическим током стенки. На определенном расстоянии от стенки в пределах тонкого слоя температура жидкости, как правило, возрастала и снижалась в области больших волн. Обнаружены пульсации температуры в больших волнах, вызванные турбулентными вихрями и относительным движением жидкости между волной и подложкой. С помощью статистических методов обрабатываются результаты измерений с целью установления взаимосвязи между толщиной пленки и температурой жидкости при различных значениях числа Рейнольдса пленки и теплового потока. При высоких значениях теплового потока связь между этими двумя величинами является более сильной, чем при низких. Анализ спектров отчетливо показывает наличие полосы частот, характеризующейся взаимосвязью двух указанных параметров.